Effect of Transcytolemmal Water Exchange in DCE-MRI Data Analysis of Human Head and Neck Cancer

S. Kim[1], H. Quon[2], L. A. Loevner[1], M. Rosen[1], A. M. Kilger[1], J. D. Glickson[1], H. Poptani[1]

[1]Radiology, University of Pennsylvania, Philadelphia, PA, United States, [2]Radiation Oncology, University of Pennsylvania, Philadelphia, PA, United States

Introduction: Dynamic contrast enhanced-MRI (DCE-MRI) of a diffusible tracer can be a useful tool for diagnosis of cancer and monitoring treatment response with antiangiogenic and neoadjuvant therapies. The dynamics of contrast reagent (CR) uptake has often been analyzed using the Kety-Schmidt two-compartment model assuming that the trancytolemmal water exchange always satisfies the fast exchange limit (FXL) [1]. Recently, it has been demonstrated in animal tumor models that deviations from the FXL model occur when the bolus of contrast agent first arrives at the target tissue [2, 3]. However, this analysis has not been reported in human head and neck cancer. The present study was conducted to evaluate the significance of variations in transcytolemmal water exchange in the quantitative analysis of CR uptake in human squamous cell carcinoma of the head and neck.

Method: The human study was approved by the IRB, and written informed consent was obtained from all subjects (n = 3) prior to the scans. T2 weighted images (TR/TE = 2 s/13 ms) were acquired initially to locate the tumor lesion. Prior to initiation of the DCE-MRI experiment, a T1 map of the tissue was constructed using an inversion recovery prepared turbo FLASH 3D sequence with 5 different inversion times. A fast 3D gradient-echo sequence was modified to acquire eight angle-interleaved sub-aperture images from the full-echo radial data [4]. This strategy provides flexibility to reconstruct images with various spatial and temporal resolution. Data acquisition was performed on a 1.5T Siemens Sonata scanner (Siemens Medical Systems, Iselin, NJ) with a neck array coil. The imaging parameters were: 256 readout points, 256 views (32 views/subaperture, 8 subapertures), FOV = 26 cm, slice thickness = 5 mm, 8 axial slices, flip angle = 20˚, receiver bandwidth = 510 Hz/pixel, TR = 5.0 ms, and TE = 4.2 ms. The scan time of each acquisition was about 20 s with fat and spatial saturation. This data acquisition scheme allows us to achieve 2.5 s temporal resolution for each sub-aperture image. Baseline pre-injection images were acquired for 1 minute. 0.1 mM/kg Gadodiamide (Omniscan; Nycomed) was injected at 1 mL/s into an antecubital vein, followed by saline flush with a power injector (Medrad, Idianola, PA), during which scanning was continued for another 9 minutes. Using the KWIC method [4] and motion correction [5], high spatial resolution images were reconstructed with 2.5 s temporal resolution.

The pharmacokinetic analysis requires knowledge of arterial input function (AIF). The AIF was obtained from the carotid artery located close to the tumor lesion as shown by a small ROI (a) in Fig.1. Since the temporal resolution is high enough (2.5 s) to describe the AIF as shown in Fig.2a, we used the average signal of the ROI as the AIF, instead of using a numerical model fitted to the measured data. Data analysis was performed using two variants of the BOLERO model of Yankeelov et al. [6]: 1) the FXL-constrained model assumes that the FXL applies throughout with transfer constant K^{trans} and extravascular extracellular space, v_e. 2) The FXR-allowed model allows for deviations from the FXL when the CR bolus first arrives at the tumor, but assumes that the FXL otherwise is applicable. The latter model fits data to the parameters K^{trans}, v_e, and mean intracellular water molecule lifetime τ_i. The parameters held constant during the analysis were hematocrit (0.5), tissue water volume fraction (0.8), interstitial and blood CR relaxivity (4.5 $mM^{-1}s^{-1}$), and blood T1 (1.35 s) based on the literature data [1,2,6]. The regions of interest (ROI) for the tumor core (c) and rim (r) were drawn as shown in Fig.1. The mean data profile of each ROI was used to fit to both FXL and FXR models using the measured AIF. The model parameters were estimated using the Simplex method by minimizing the mean square difference between the data and the model. The goodness of fit was evaluated using Chi-square statistics. Image reconstruction and data analysis software were developed using IDL (RSI, Boulder, CO).

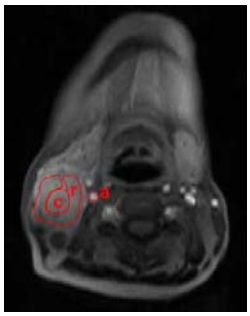

Fig.1 Representative ROIs shown on a T1-weighted image after CR injection.

Results and Discussion: Representative mean ROI data from Fig1 are shown in Fig.2a. The temporal resolution of the data is high enough to delineate the fast change in the AIF adequately. The model fitting results are depicted in Fig.2b and c. The estimated parameters for all three subjects are given in Table 1. For the core regions, both the FXL-constrained and FXR-allowed models appear to fit the data well. χ^2 in Table 1 shows that the FXR-allowed model fits better than the FXL-constrained model. For the rim regions, noticeable mismatch between the data and the FXL-constrained model was consistently observed with all subjects. On the other hand, the FXR model was able to fit the data well, particularly on the rising edge. The improvement in the goodness of fit can be noticed from χ^2 in Table 1. The K^{tans} and v_e estimated by the FXR-allowed model are larger than those estimated by the FXL-constrained model. The rim region appears to have better perfusion than the core region. These observations and the estimated parameter values are in good agreement with previously reported observations from animal studies [2, 3, 6]. The overall result indicates that the FXR-allowed model can represent the measurement data more adequately than the FXL-constrained model. To conclude, our preliminary result suggests that DCE-MRI data of human head and neck cancer can be more accurately represented by the FXR-allowed model, which includes transcytolemmal water exchange.

Table 1. Pharmacokinetic parameters from BOLERO analysis of DCE-MRI data

		K^{trans}		v_e		τ_i (s)	χ^2	
Subject		FXL	FXR	FXL	FXR	FXR	FXL	FXR
Core	1	0.10	0.13	0.27	0.56	0.38	1.48	0.75
	2	0.03	0.05	0.06	0.29	2.95	0.23	0.13
	3	0.16	0.19	0.28	0.53	0.66	0.69	0.31
Rim	1	0.18	0.29	0.27	0.53	0.36	2.24	0.38
	2	0.45	0.89	0.33	0.68	0.59	3.96	0.39
	3	0.36	0.48	0.31	0.69	0.74	1.90	0.46

References: [1] Tofts et al., JMRI 10:223-232, 1999. [2] Landis et al., MRM 42:467-478, 1999. [3] Zhou et al. MRM 52:248-257. [4] Song and Dougherty, MRM 52:815-824, 2004. [4] Kim et al. ISMRM 229, 2005. [6] Yankeelov et al., MRM 50:1151-1169, 2003.

Acknowledgement: This study was funded by the NIH grant RO1 CA102756-01A1.

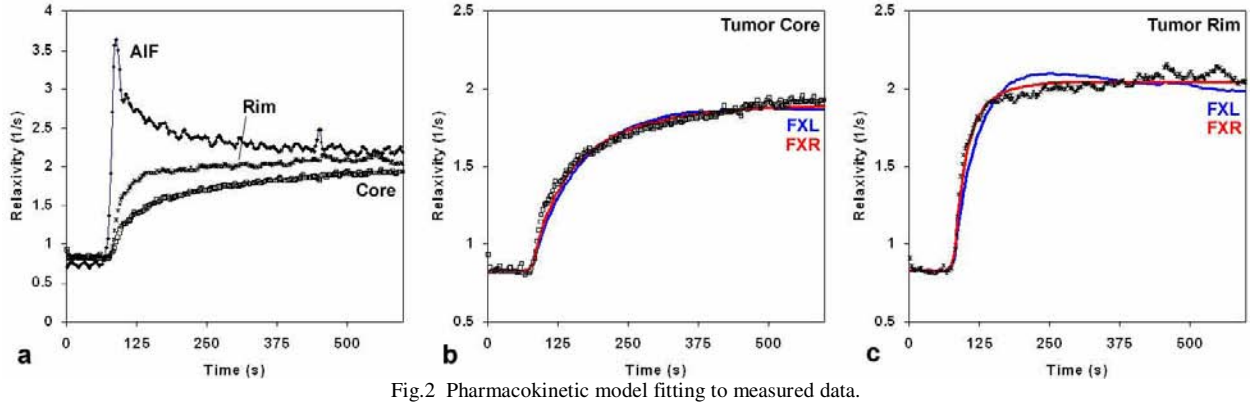

Fig.2 Pharmacokinetic model fitting to measured data.